Pharm Res (2011) 28:1431–1441
DOI 10.1007/s11095-010-0321-5

RESEARCH PAPER

A Novel Shell-Structure Cell Microcarrier (SSCM) for Cell Transplantation and Bone Regeneration Medicine

Kai Su • Yihong Gong • Chunming Wang • Dong-An Wang

Received: 30 September 2010 / Accepted: 3 November 2010 / Published online: 19 November 2010

ABSTRACT

Purpose The present study aims to develop a novel open and hollow shell-structure cell microcarrier (SSCM) to improve the anchorage-dependent cell (ADC) loading efficiency, increase the space for cell proliferation and tissue regeneration, and better propel its therapeutic effects.

Methods Gelatin particles were prepared with oil/water/oil (o/w/o) technique and modified by an adjustable surface crosslinking technique and subsequent release of uncrosslinked material. Optical microscopy and scanning electron microscopy (SEM) were utilized to observe the morphologies of the microcarriers. Cell loading tests were performed to evaluate the biocompatibilities and effect on osteogenesis of SSCM.

Results SSCMs were successfully fabricated via the surface technique. The shell-structure could allow the cell to attach and grow on both outer and inner surface of sphere and provide adequate space for cell proliferation and extracellular matrix (ECM) secretion. The cell loading rate, proliferation rate and osteogenesis-related gene expressions on the SSCMs were higher than those on the spherical gelatin microcarriers.

Conclusions The outstanding performance of injectable SSCMs endowed with favorable micro-structure, desirable cytocompatibility and enhanced cell affinity makes them as a good choice as cell delivery vehicle for transplanting therapeutic cells towards the scope of tissue regeneration.

Y. Gong (✉)
Department of Biomedical Engineering, School of Engineering
Sun Yat-sen University
Guangzhou 510275, China
e-mail: Gongyih@mail.sysu.edu.cn

K. Su • Y. Gong • C. Wang • D.-A. Wang
Division of Bioengineering
School of Chemical and Biomedical Engineering
Nanyang Technological University
Singapore 637457, Republic of Singapore

KEY WORDS cell therapy · gelatin · microcarrier · regenerative medicine

INTRODUCTION

Therapeutic cell transplantation, which has drawn increasing attention and has become more and more important in regenerative medicine in the recent decade, requires that the cell-laden vehicles with conveyable and vast cell-loading interfaces can be injected into the targeted site *in vivo* and degrade after therapy (1–4). Since anchorage-dependent cells (ADCs) are a major family of therapeutic cell species, the cell microcarriers also need appropriate surface characteristic to support cell proliferation and ensure intact cell phenotype during the delivery (5–7). For this purpose, biodegradable materials, including synthetic or natural polymers such as PLLA, PLGA, dextran, gellan and collagens, were fabricated into microspheres (3,8–13). Because of the advantages of microcarriers for injectable mass conveyance and the unique focal adhesional accommodation for ADCs, the researchers have continuously focused attention on the development of novel vehicle models to pursue better delivery efficacies. A major challenge of the microcarrier for transplantation of therapeutic cells is that in microcarrier culture, cells grow mainly on the spherical surface as monolayers or in the pores of macroporous structures (14,15). Even for the macroporous microcarrier, it is difficult for cells to penetrate certain pores whose diameter is slightly bigger than that of cells (for example, cytopore^{TM} <30 μm (16)) and to grow into the core region. Therefore, a large amount of unnecessary spherical substance has to be introduced into the body together with therapeutic cells in order to achieve adequate amount of cells. The ultra large amount of microcarrier

substance or degraded product may induce medical risks such as rejection, inflammation or other immune reactions. Furthermore, the microcarrier bulk without cells will occupy most of the volume in the injection system, which may limit cell proliferation, extracellular matrix (ECM) secretion and tissue regeneration.

In this study, we invented a novel open and hollow shell-structure cell microcarrier (SSCM), which allows the cells to attach and proliferate on both outer and inner surface of the microcarrier. Spherical gelatin spheres were modified and fabricated to SSCMs via a special surface crosslinking progress which can effectively control the dissolution fate of gelatin spheres and significantly provide the basis for SSCM forming. Scanning electron microscopy (SEM) was employed to visualize the shell-like structure of the resultant microcarrier. Cell loading tests were performed to evaluate the biocompatibilities and effect on osteogenesis of SSCM.

MATERIALS AND METHOD

Materials

All reagents unless otherwise specified were purchased from Sigma-Aldrich Inc. and used as received.

Preparation of Gelatin Spheres

Gelatin (4 g) was dissolved in distilled water (40 mL) at 70°C and poured into a 100 mL beaker. Ethyl acetate (20 mL) was added into the solution. After vigorous stirring for 2 min with mechanical stirrer at 700 rpm, the mixture was quickly poured into 60 mL peanut oil under agitation at the rate from 300 rpm to 400 rpm. After being stirred at room temperature for 15 min, the mixture was then cooled down to ~4°C by a −10° C ice-salt bath. The stirred suspension was poured into 500 mL alcohol, which was pre-cooled in −20°C refrigerator. After 5~10 min, the gelatin spheres were deposited and then washed by 1,4-dioxane and acetone each three times to remove residual peanut oil. The washed gelatin spheres were air-dried in 70°C and separated by standard sieve. Gelatin spheres with diameters of 100~154 and 180~280 μm were separated and utilized for preparation of SSCMs.

Gelatin Sphere Reshaping and Preparation of SSCMs

Gelatin spheres with diameter of 100~154 and 180~280 μm were reshaped by ethanol solution to generate shell-like structure. Briefly, the gelatin spheres (0.5 g) were added into a 24-well plate, and the plate was tapped gently to make a flat surface of the gelatin particles, followed by a slight pressing. Eight-five percent alcohol solution (~0.5 mL) was then added into gelatin spheres slowly by a syringe. The plate was transferred to an oven at 70°C and heated for 5~8 min to make the gelatin spheres swell. The plate was then taken out and cooled down to room temperature for 30 minutes before drying by vacuum. To determine the packing density of the gelatin spheres before and after reshaping, the samples with weight (W) were added into a precisely graduated cylinder and shaken to make the spheres pack closely. The packing density is calculated by $\rho' = W/V'$, where V′ is the packing volume of gelatin spheres.

The glutaraldehyde aqueous solution (25%, w/w) was diluted 10 times by ethanol and added into the dried reshaped gelatin spheres. The mixture was kept at 4°C for 24 h in order to crosslink the surface of gelatin spheres. Then, the microspheres were separated, washed by ethanol six times and heated at 100°C for 2 h. The dried microspheres were added into PBS at 37°C for 30 min; the shell-like structure could be obtained as the result of swelling, expansion and dissolution of the uncrosslinked material. The products (SSCMs) were washed by PBS three times, and stored at 4°C for further use.

As a control, spherical gelatin microcarriers (180~280 μm) were also prepared via a similar method by using the gelatin spheres without sphere reshaping.

Crosslinking Ratio

To obtain the crosslinking ratio, the weight of crosslinked microspheres (W_0) was measured. After swelling in water, the shell-like structure finally formed, and the microcarriers were separated and lyophilized for dry weight ($W_{crosslinked}$) measurement. The crosslinking ratio is calculated by $W_{crosslinked}/W_0 \times 100\%$.

Cell Culture

Human fetal osteoblasts (hFOBs 1.19) were purchased from American Type Culture Collection (ATCC, Manassas, VA, USA) and cultivated in DMEM/Ham's F12 (1:1) culture medium with the supplements of with 2.5 mML-glutamine, 0.3 mg/mLG418 and 10% (v/v) FBS. All these cell culture-related reagents were purchased from Gibco (Invitrogen, Singapore).

Cell Seeding

For microcarrier cultural purpose, microspheres were sterilized by soaking and rinsing in a penicillin and streptomycin solution (1000 μg/mL and 1000 units/mL in PBS) for 24 hrs and subsequently equilibrated in cell culture medium for 4 h. The cell seeding process was conducted in a sterilized 1.5 mL *eppendorf* tube. First, the microcarriers (SSMC: 5 mg and gelatin spherical micro-carrier: 75 mg, dry weight) were added into the tube. Then,

500,000 hFOBs (suspended with 0.5 mL medium) were mixed with the microcarriers and cultivated for 8 h for cell attachment on the microcarrier. The *eppendorf* tube can be placed vertically to confine cells and microspheres inside for well cell seeding. Then, the microcarriers were transferred carefully to a cell strainer with pore size of 40 μm and cultivated in a six-well plate. The temperature of incubation was set differently at 33.5°C for proliferation during the first seven days and 39.5°C for osteogenic differentiation for another seven days (17).

Cell Number Determination and Cell Viability Observation

After proliferation for seven days, the cell number determination was carried out via Hoechst assay (Hoechst 33258, Molecular probes, Invitrogen), following the manufacturer's instructions. DNA quantities of the specimens were measured, and the committed cells numbers could be calculated via a conversion rate of 6.6 pg DNA per cell (18). The loaded cell viability on the microcarriers was observed on Day 7 using a Live/Dead assay (Molecular probes, Invitrogen Singapore) following the manufacturer's instruction.

Scanning Electron Microscopy (SEM)

SEM (Stereoscan 260, Cambridge and JSM-6700F, JEOL Ltd., Tokyo, Japan) was used to observe the morphology of the microcarriers and the attached cell morphology at Day 7. Briefly, the cell-laden microspheres were fixed and preserved by glutaraldehyde (2.5%, 4°C, 1 h) and then pre-treated with 1% OsO_4 at 4°C for 2 h. The specimens were dehydrated in gradient ethanol solutions and further dried in vacuum overnight, before being coated with platinum SEM contrasting.

Immunocytochemistry

FITC-labeled anti-integrin α5 and PE-labeled anti-integrin β1were used to evaluate the expression of a pair of integrins on microcarriers at protein level. Briefly, the cell-laden microcarriers were fixed by paraformaldehyde (4%, 20 minutes), permeabilized with 0.1% Triton X-100 and blocked with 1% BSA, based on which different antibodies were separately applied to indicate integrin α5 (green) and β1 (red). Similarly, F-actin in spreading hFOBs was detected on Day 7 using FAK100 cytoskeleton and focal adhesion kit (Chemicon, Temecula CA, USA). After the pretreatments, the TRITC-conjugated Phalloidin was applied to label F-actin, and the cell nuclei were also counterstained by DAPI. Fluorescent microscopy was employed for the observation of the stained samples. In order to detect the framework of F-actin, the F-actin-labeled samples were also observed by a confocal laser scanning microscopy (CLSM).

Osteogenic Indications and Real-Time Quantitative Reverse Transcription-Polymerase Chain Reaction

After seven days proliferation stage, the hFOBs were cultivated under 39.5°C for another one week to induce osteogenesis. The cells were harvested at Day 14 and subjected to alkaline phosphatase (ALP) assay. The ALP was measured using pNPP assay (p-nitrophenyl phosphate liquid substrate, Sigma Diagnostics) following the manufacturer's instructions, and normalized against cell numbers which were detected by Hoechst assay (Hoechst 33258, Molecular probes, Invitrogen) (18). Calcium blue solution (30 μM, 37°C, and 10 min) was applied to determine the deposit of calcium on the microcarrier. After staining, the samples were subjected to fluorescent microscopy for observation.

Total RNA of the hFOBs at Day 14 was isolated by following TRIzol protocol (19) and subjected to reverse transcription (RT) with SuperScript™ First-Strand Synthesis System (Promega,USA) (20). The gene expressions of ALP, Osteocalcin (OC), Osteopontin (OPN), Collagen I and β-actin were detected from the yielded complementary DNA (cDNA) by PCR examining. The adopted primer sequences are listed in Table 1 (20). The quantitative polymerase chain reaction (qPCR) was conducted with SYBR green assay (iQ supremix, Bio-rad). The gene expressions were quantified with a calculation of $2_{\mathrm{T}}^{-\Delta C}$, where C_T represents the cycle number when an arbitrarily placed threshold was reached, and $\Delta C_T = C_{T,\mathrm{targetgene}} - C_{T,\mathrm{b-actin}}$).

Statistical Analysis

Where appropriate, ANOVA was performed to analyze results, and a $P<0.05$ was considered to indicate a

Table 1 Validated Primer Sequences for Real-Time PCR

Gene	Direction	Sequences(5′- 3′)
ALP	Forward	GGGAACGAGGTCACCTCCAT
	Reverse	TGGTCACAATGCCCACAGAT
Osteocalcin (OC)	Forward	AGCAAAGGTGCAGCCTTTGT
	Reverse	GCGCCTGGGTCTCTTCACT
Osteopontin (OPN)	Forward	ACCTGAACGCGCCTTCTG
	Reverse	CATCCAGCTGACTCGTTTCATAA
Collagen I	Forward	CCTGCGTGTACCCCACTCA
	Reverse	ACCAGACATGCCTCTTGTCCTT
β-actin	Forward	CCTGGCACCCAGCACAAT
	Reverse	GGGCCGGACTCGTCATACT

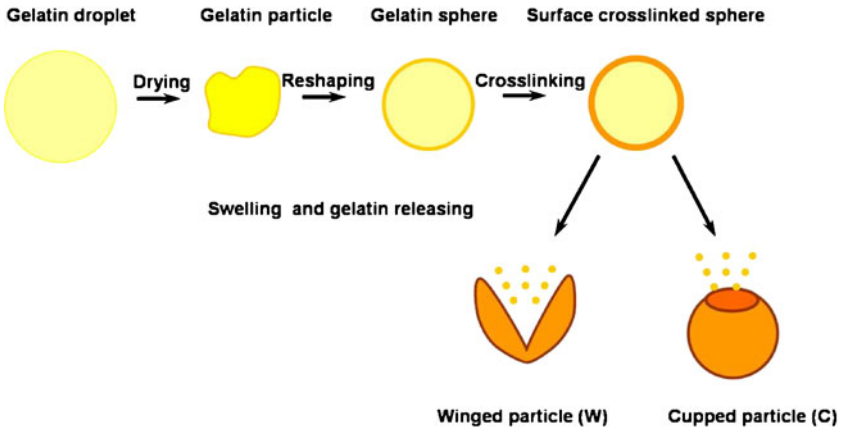

Fig. 1 Schematic diagrams of fabrication of SSCMs: Gelatin spheres were prepared by o/w/o method and shrunk during the drying process. After reshaping, the gelatin spheres were recovered to spherical shape with a smooth and compact surface. The surface of gelatin spheres was fixed by glutaraldyhyde ethanol solution, and SSCMs were obtained as the result of removal of uncrosslinked substance by water.

statistically significant difference. Data are presented as mean ± SD.

RESULTS

Morphology of Gelatin Spheres

The gelatin spheres were prepared by double emulsion method as demonstrated in Fig. 1. The diameter distribution was greatly influenced by the stirring rate. Along with the increase of stirring rate from 300 to 400 rpm, the percentage of spheres with smaller diameters increased (Fig. 2). The morphologies of the microspheres were exhibited in Fig. 3. Most of the gelatin spheres were obviously shrunken, and small pores or grooves could be easily observed on the surface of spheres (Fig. 3b and d), which is probably due to the evaporation of ethyl acetate and following drying process.

Formation of SSCMs

In order to regain the spherical morphology and obtain a smooth and compact surface, the reshaping process was performed via hot ethanol solution treatment. As shown in Fig. 4a and b, the morphology of gelatin sphere could rapidly recover to spherical shape after being placed into 85% ethanol aqueous solution at 70°C. The SEM images (Fig. 4c~e) show that after the reshaping progress, most of the gelatin spheres retained their spherical shape. The small

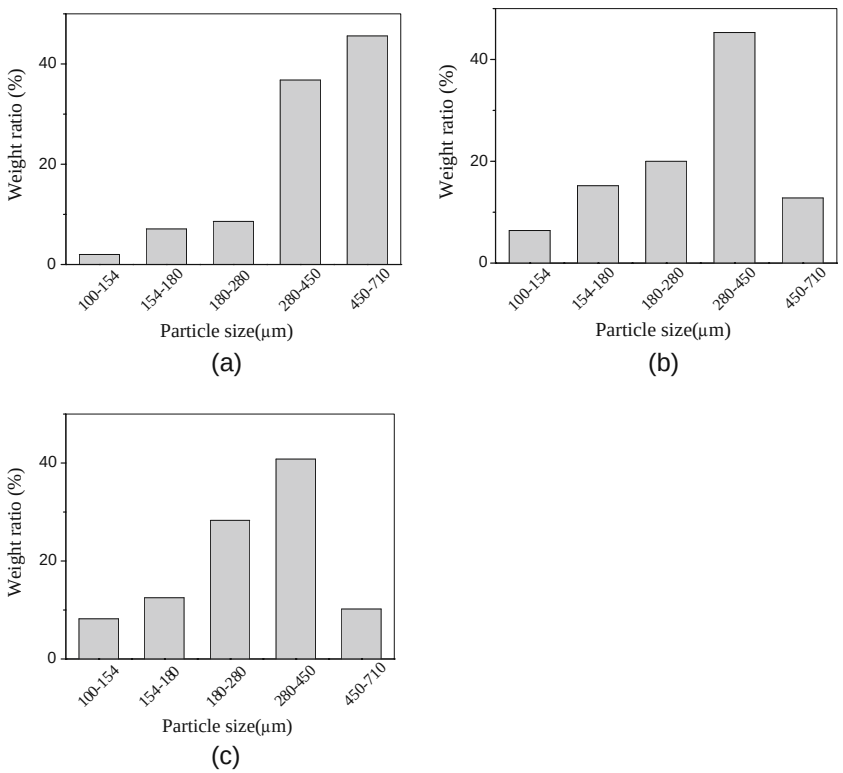

Fig. 2 Particle size distribution histograms of the gelatin microspheres fabricated at different stirring rates: **a** 300 rpm, **b** 375 rpm and **c** 400 rpm.

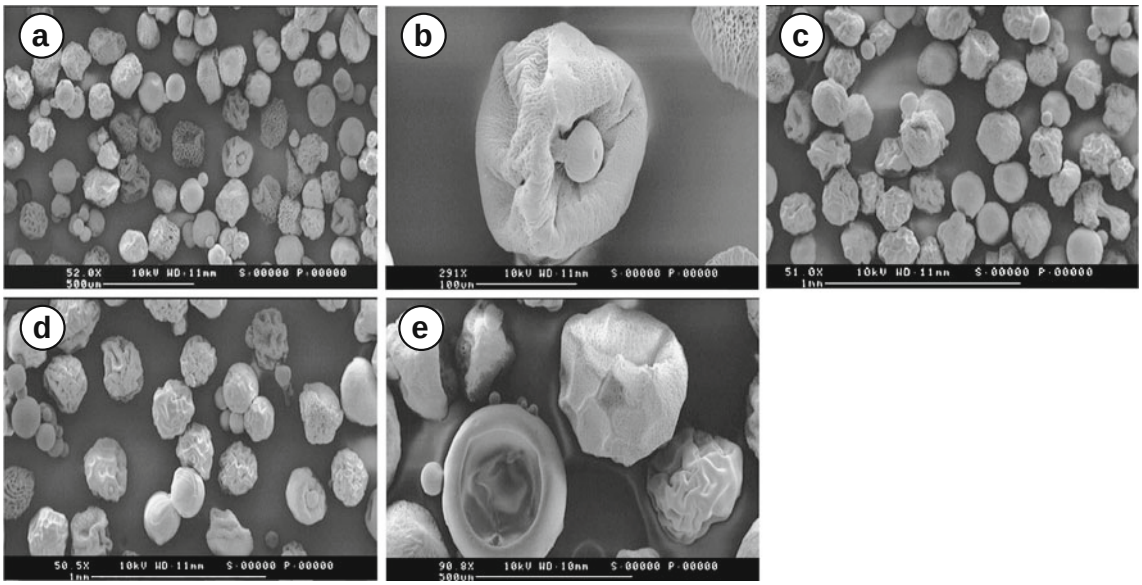

Fig. 3 SEM images of gelatin spheres with different diameter: **a** 100~150 μm; **c** 150~180 μm; **d** 180~280 μm and **e** 280~450 μm, **b** is a magnified image of (**a**).

pores and grooves disappeared, and the surface became smooth and compact. The change of sphere morphologies led to the decrease of sphere packing densities. The packing density of gelatin spheres with diameter of 100~154 μm shifted from 0.63 ± 0.02 to 0.58 ± 0.02 g/cm^3, and that of gelatin spheres with diameter of 180~280 μm changed from 1.0 ± 0.03 to 0.59 ± 0.03 g/cm^3, which indicated the shape change of the microspheres.

Glutaraldehyde ethanol solution was employed to crosslink the surface of microspheres after reshaping. Figure 4f shows that after crosslinking, the microspheres retained their spherical shape, but the sphere surface became a little rough. After swelling in PBS at 37°C for a very short period of time, most of the spheres were broken by their internal pressure, and the uncrosslinked material was dissolved and released. Then, the shell-structure cell microcarriers

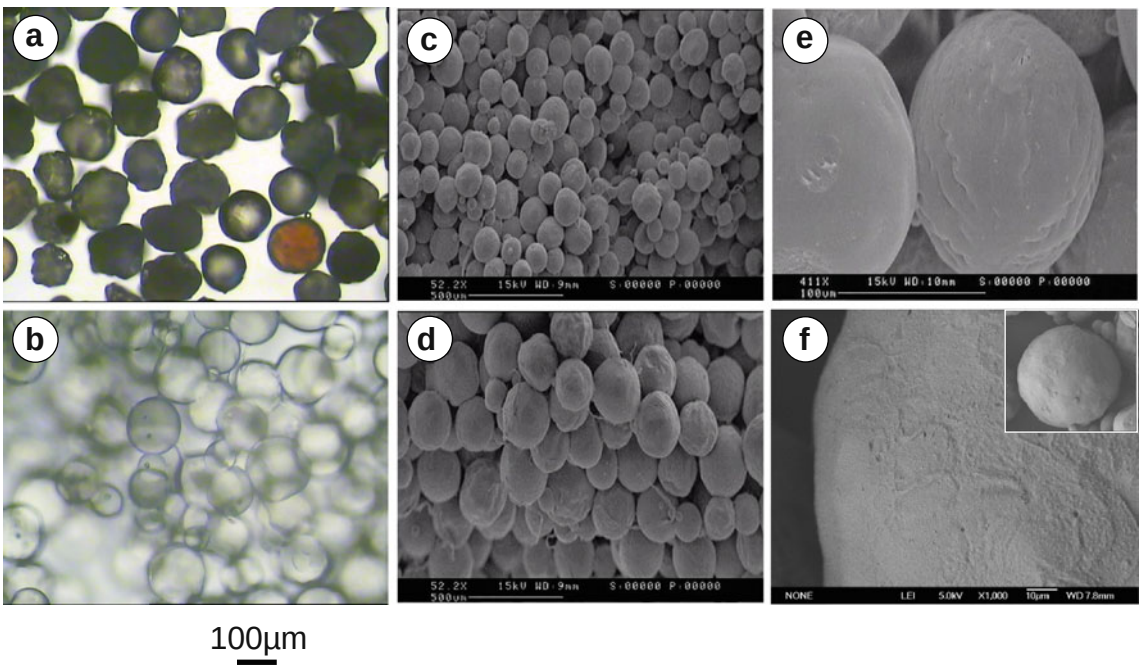

Fig. 4 Optical microscopic observation of gelatin spheres **a** before reshaping in ethanol aqueous solution at 70°C; **b** after reshaping; SEM images of gelatin spheres after reshaping with different diameter: **c** 100~150 μm; **d** 150~180 μm; **e** is magnified image of (**c**); and **f** SEM images of gelatin spheres after surface crosslinking.

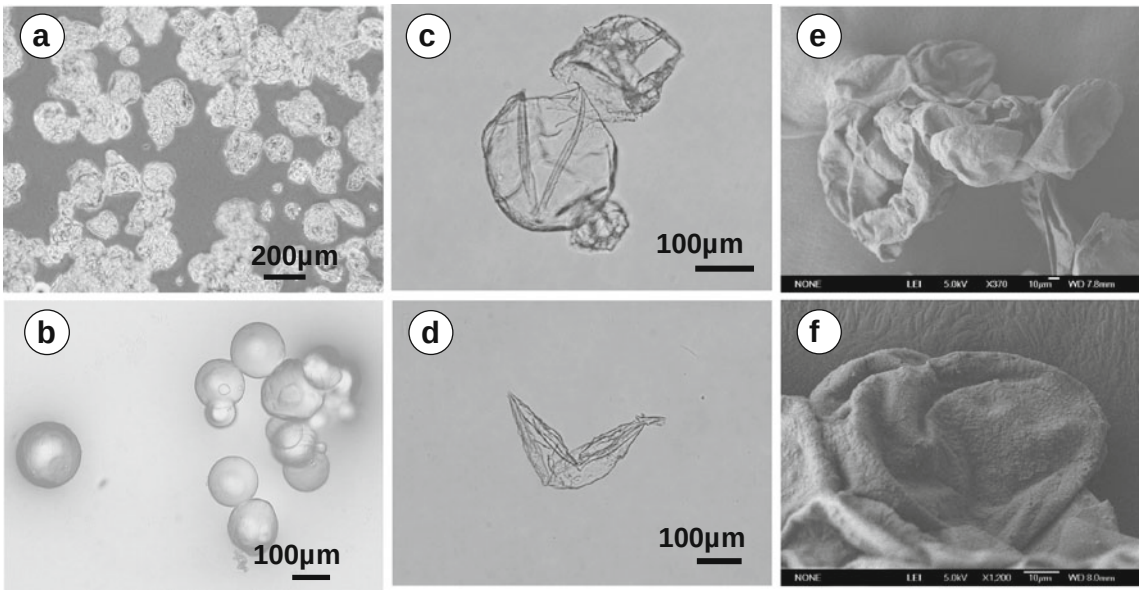

Fig. 5 Optical microscopic morphology of microcarriers: **a** SSCM (180~280 μm); **b** gelatin spherical microcarrier; **c** cup-like microcarrier; **d** wing-like microcarrier; and **e** SEM images of SSCM (180~280 μm); **f** is magnified image of (**e**).

(SSCMs) with winged or cupped morphology were finally obtained (Fig. 5a, c, d). On the other hand, most of the spheres without reshaping treatment retained their spherical morphology under the same condition. After drying, the morphologies of SSCMs were observed by SEM (Fig. 5e and f). The surface of SSCMs became very rough, and the SSCMs tended to aggregate with each other. The crosslinking ratios are shown in Table 2, which indicated most of sphere material (about 95%) was released during the swelling progress of SSCM preparation. The thickness of the sphere shell was about 1~2 μm via measuring from Fig. 6a.

Cell Adhesion

Live/Dead staining indicates that a large number of hFOBs with high viable adhesion on the surface of SSCMs and only very few dead cells were observed (Fig. 7a). Furthermore, SEM images show that the hFOBs could live on the both outer and inner surface of carriers (pointed out by the white arrow in Fig. 6a and b). After seven days culture, the hFOBs and SSCMs tended to aggregate with each other, and the cell growth induced microcarrier conglutination. The hFOBs, focal adhesion on SSCMs substrate was successfully manifested with immunofluorescent staining, specifically, the major focal contacting indicators, including the oriented F-actin, integrin-α5 and integrin-β1, which could be easily found in Fluorescent microcopy images (Fig. 7c, e, b and f). CLSM image (Fig. 7d) confirms the assembly of F-actin and the formation of framework.

Cell Proliferation

The number of hFOB laden on the microcarriers was kinetically monitored with DNA assay in the proliferation stage under 33.5°C. It is shown that the microcarriers with shell-structure could carry apparently more cells than the spherical microcarriers. The cells proliferated more than two times from Day 3 to Day 7 on the SSCM (100~154 μm) and SSCM (180~280 μm), while cell number on the control samples only increased about 131% (Table 2).

Table 2 Crosslinking Ratio, Cell Load Density After and ALP Secretion of SSCMs and Control Samples. Differences Between Different Microcarriers at Same Culture Time are Significant ($p < 0.05$)

Sample	Crosslinking ratio (%)	Cell loading rate ($\times 10^3$cell per mg dried microcarriers)		ALP secretion (Unit/L per million cells) after osteogenesis Day 14
		Day 3 proliferation	Day 7 proliferation	
SSCM (100~154 μm)	5.2 ± 0.3	72.5 ± 0.5	223.7 ± 4.6	3.2 ± 0.8
SSCM (180~280 μm)	4.5 ± 0.2	77.1 ± 0.8	361.2 ± 7.2	4.7 ± 0.6
Spherical microcarriers (Control)	75 ± 1.2	9.69 ± 0.2	22.4 ± 0.8	2.8 ± 0.6

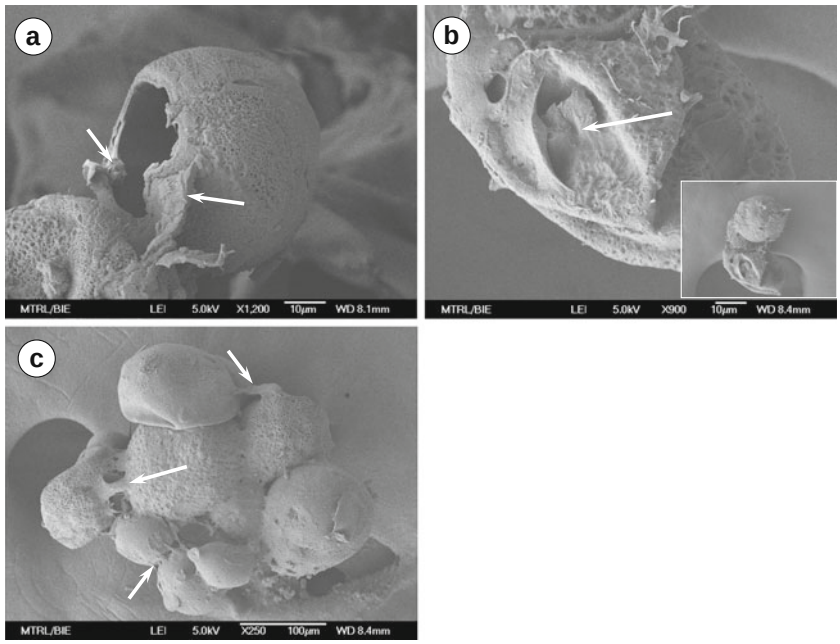

Fig. 6 SEM observation of hFOBs cultivated on the SSMC (180~280 μm) after 7 days proliferation: **a** cup-like microcarrier with cells on both outer and inner surface as the white arrows pointed out; **b** wing-like microcarrier with cells on the surface; **c** cell growth-induced intermicrospherical conglutination.

Early Osteogenesis and Maturation

The cultural conditions were altered for differentiation purpose by elevating the cultivation temperature to 39.5°C (18) and lasting for another seven days. Positive ALP production and osteogenesis gene expression were detected at Day 14 (Table 2 and Fig. 8). Accordingly, significant mineralization was detected via fluorescent staining, and higher calcium fluorescent signals (blue) were observed in SSCM (100~154 μm) and SSCM (180~280 μm) (Fig. 9). The heavier calcium blue fluorescent staining marked the higher extent of mineralized nodule formation in hFOBs culture on SSCMs.

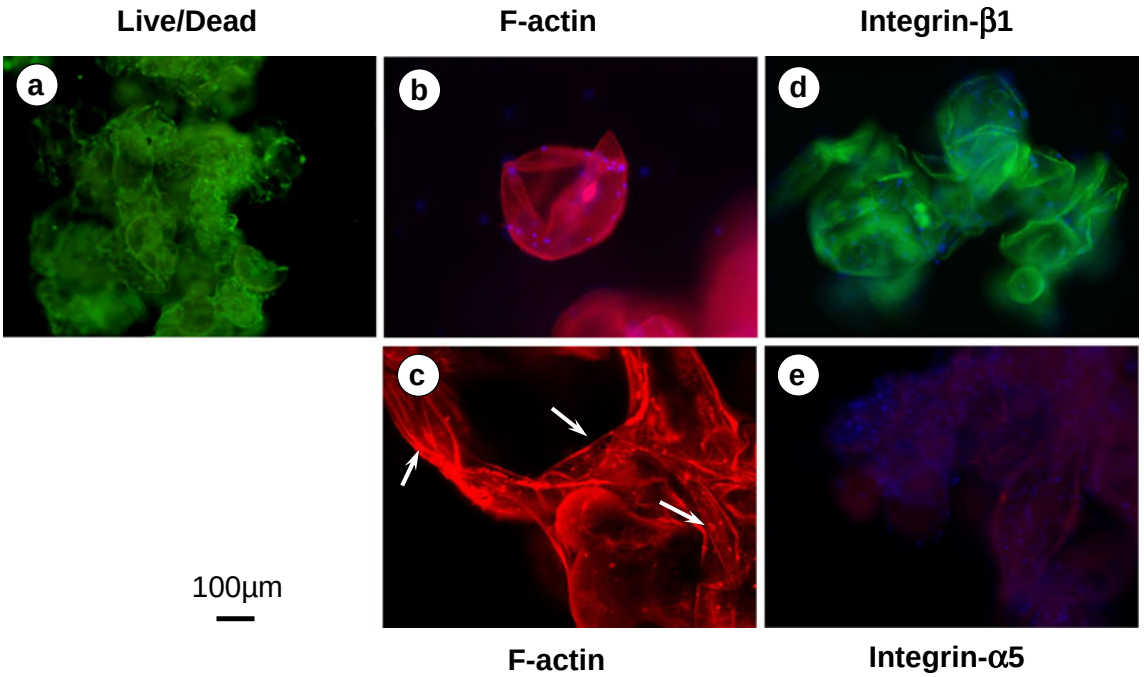

Fig. 7 **a** Live/Dead staining of hFOBs laden on SSCM (180~280 μm); Immunofluoresent staining of hFOBs cultivated on the microcarriers: **b** TRITC-phalloidin for F-actin (*red*); **d** PE-labeled anti-integrin β1 for integrin β1 (*green*); **e** FITC-labeled anti-integrin α5 for anti-integrin α5, and nuclei was counterstained by DAPI for (*blue*); and **c** CLSM images of hFOBs laden on SSMC (180~280 μm) after 7 days proliferation.

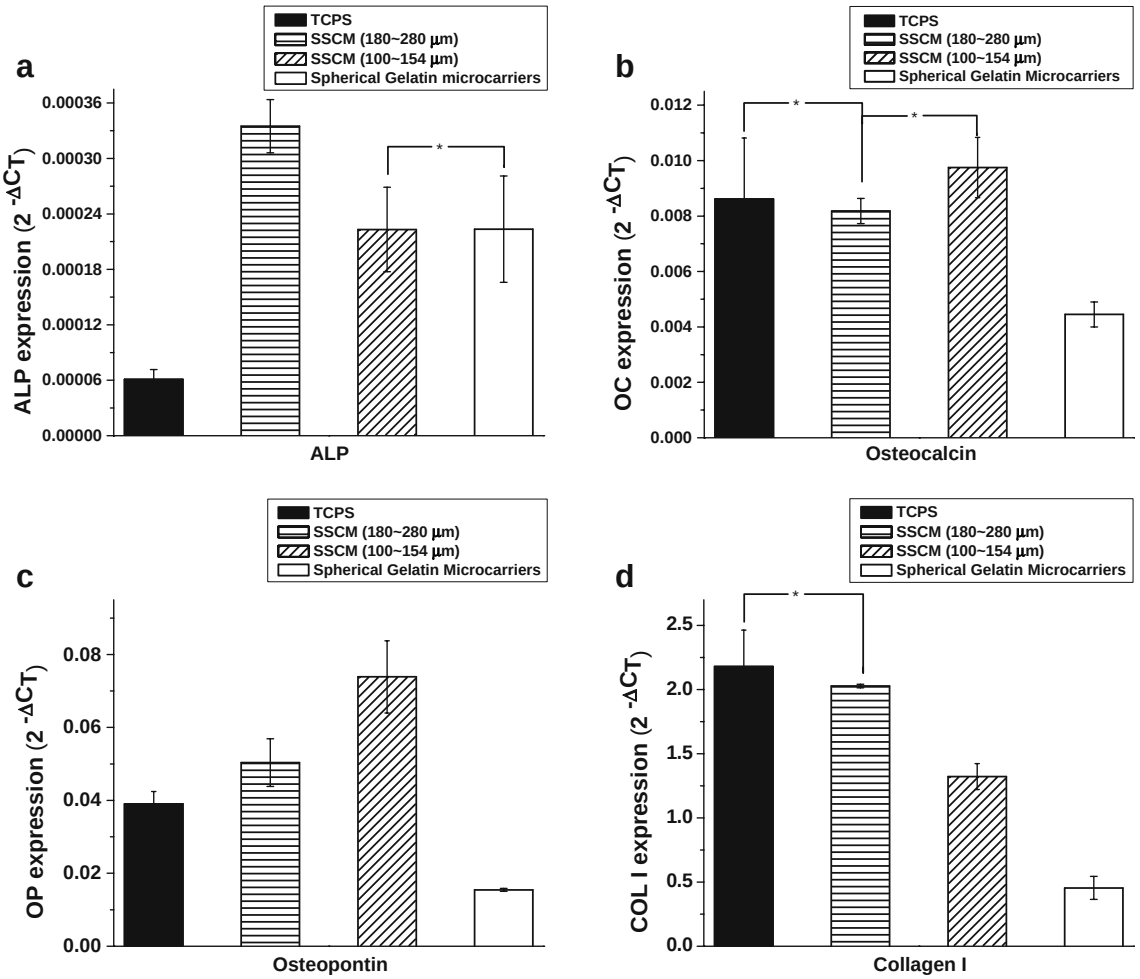

Fig. 8 Gene expression of **a** ALP; **b** osteocalcin (OC); **c** Osteopontin (OPN) and **d** Collagen I using real-time PCR after osteogenesis (Day 14). Differences between different samples at the same culture time are significant except labeled by *.

DISCUSSION

The practice of rapid large-scale *ex vivo* expansion, cell transplantation and tissue engineering highly demands competent cell vehicles. The characteristics of cell microcarriers play a key role in controlling cell quality and quantity, which will exert critical influence on the actual functionality of the overall treatment (12). In this study, we invented a novel microcarrier with shell-structure for *ex vivo* cell expansion and injectable cell transplantation. SSCM is modified from traditional spherical microcarrier, and it has an open hollow structure, which decreases the mass of microcarrier effectively and allows the cell to grow on both outer and inner surface of the microcarrier.

The key of SSCM manufacturing is to control the crosslinking reaction to only occur on the sphere surface. For this purpose, double emulsion method was utilized to prepare the gelatin sphere, which will make the sphere structure loose and easy to handle for reshaping. We have made an attempt to use single emulsion to prepare the gelatin sphere, but the compact structure will absorb water and expand badly during the reshaping, which makes the progress hard for controlling. Due to the escape of ethyl acetate and dehydration, the gelatin sphere shrunk to irregular shape with a lot of small pore on the surface (Fig. 3). Hence, if the glutaraldehyde solution was added at the appropriate moment, the whole sphere would be crosslinked. In order to achieve a smooth and compact sphere surface, ethanol aqueous solution was added into the gelatin spheres, and the mixture was heated for 5~8 min. As shown in Fig. 4, the gelatin spheres could recover to their original shape, and the sphere surface became very smooth, probably due to the surface tension after drying. Then, the compact sphere surface could prevent glutaraldehyde solution from invading into the core region, and the uncrosslinked material (about 95%) would be removed by warm water. Finally, the sphere with an open, hollow, wing-like or cup-like structure was obtained (Fig. 5c and d). It is noted that gelatin sphere without reshaping could also swell into spherical shape in PBS after crosslinking (Fig. 5b),

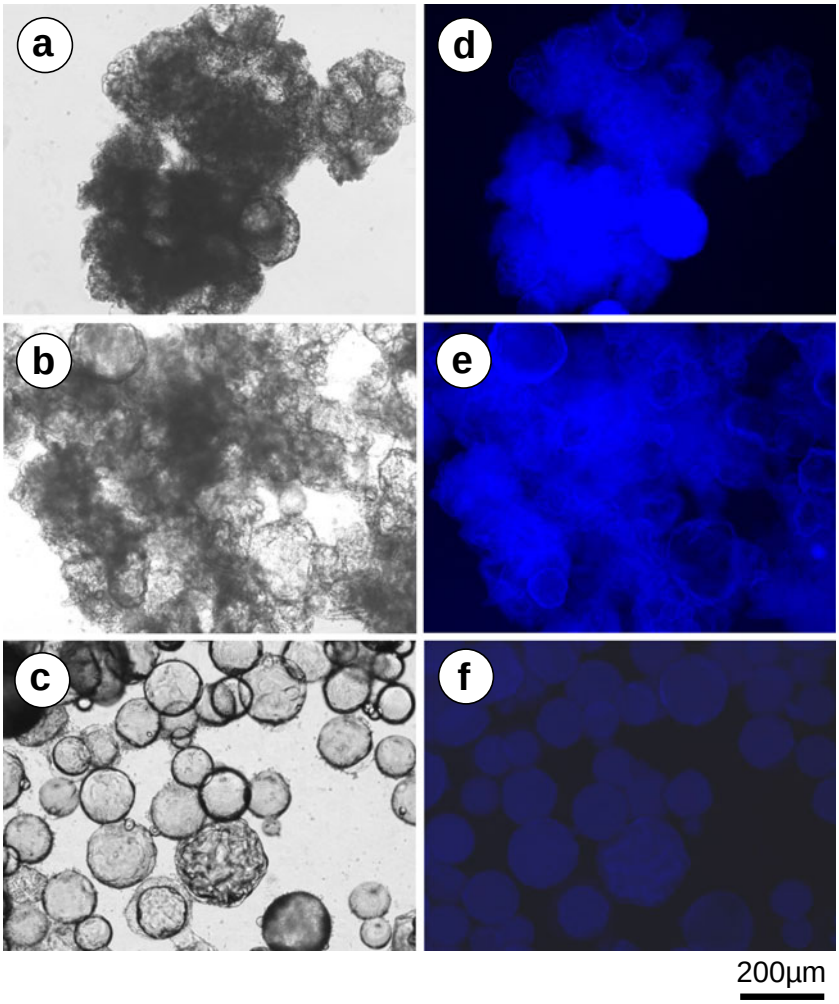

Fig. 9 Optical microscopic morphology of microcarriers: **a** SSCM (100~154 μm); **b** SSCM (180~280 μm); **c** gelatin spherical microcarrier and Calcium Blue fluorescent staining: **d** SSCM (100~154 μm); **e** SSCM (180~280 μm); **f** gelatin spherical microcarrier after osteogenesis (Day 14).

but the small pores on the sphere surface disappeared because of the swelling of gelatin molecule networks.

The gelatin spheres need to undergo a swelling process after surface crosslinking in order to obtain the unique shell structure. It requires that the crosslinked surface should be tough enough to take the pressure of gelatin swelling and expansion; otherwise, the particles may possibly be broken into small pieces. We have tried other crosslink reagents such as genipin in the initial study; however, the surface of the spheres was not stable for SSCM preparation even after crosslinking for two days. Although glutaraldehyde has cytotoxicity and is difficult to remove, the gelatin layer crosslinked by glutaraldehyde has good mechanical properties and is suitable for the manufacture. Moreover, after equilibrium process of the fabricated spheres in culture medium where abundant amino acids and serum would highly consume the aldehyde groups, the toxicity of the minute amount of residual glutaraldehyde was proved to be tolerable and has been widely utilized in protein immobilization, scaffold crosslink in biomedical field. Nevertheless, there is no doubt that the glutaraldehyde should be replaced by a safer biodegradable reagent, and we will keep seeking the upgraded method to fabricate the SSCMs with better cytocompatibility and low cytotoxicity in further study.

It is well known that most types of therapeutic cells belong to ADCs, whose survival is established upon the successful ligation between cellular integrin receptors and specific ECM protein domains. Gelatin is a denatured product of collagen; thus, it contains bioactive sequences such as RGD peptide which can be recognized and incorporated with integrin (21,22). Fluorescent staining images show obvious expression of intergrin α5 and β1 on the cell surface, which represents the cell responses via surface receptor turning-over (23). F-actin assembly is confirmed by CLSM, which ketches the induced cytoskeletal organization posing for focal adhesion (21). Due to the open hollow structure, hFOBs can attach on both outer and inner surface of the carrier as pointed out in Fig. 6a, which endows SSCMs to load more cells (Table 2). The cavity inside the SSCM can also provide cells with adequate room for proliferation and ECM secretion.

The osteogenesis characteristics of SSCMs were evaluated by ALP secretion, osteogenesis expression and Calci-

um Blue staining compared with spherical gelatin microcarriers. ALP, one of the early bone markers, was found after osteogenesis (Day 14), which suggested an evoking of osteogenesis that proceeds prior to the initiation of bony mineralization. Osteocalcin is an important late bone marker secreted solely by osteoblasts, which is also implicated in bone mineralization and calcium ion homeostasis and thought to play a role in the body's metabolic regulation. Osteopontin has been implicated as an important factor in bone remodeling (24). Specifically, research suggests that it plays a role in anchoring osteoclasts to the mineral matrix of bones. Type I collagen is a fundamental ingredient (over 90%) in the structural proteins of bone, takes the major responsibility for the tensile strength and provides templates for mineralization (18,25). It is shown that most osteogenesis indicators of cells cultured on SSCM, such as ALP secretion, key gene expression, and calcium deposit, overwhelmed those of cells cultured on spherical microcarrier, which suggests that hFOBs in SSCM culture have a better early osteogenesis (26). This is probably affected by the three-dimensional structure of the microcarrier, since the chemical component of both carriers is similar. The results indicate that the hFOBs have a better performance in osteogenesis on the rough and irregular surface, compared with the spherical surface. The shape of SSCM enables cells on different carriers to contact, combine and blend into one construct. The cell growth-induced microspherical conglutination (as shown in Fig. 9e and c), which has also been observed in other microcarrier models (10,12,27), is believed to be beneficial for the constitution of neo-tissues with better continuity and integrity. In this study, the cytocompatibility of the SSCMs with two different sizes (100~154 μm and 180~280 μm) was evaluated by cell loading test. The results showed that the SSCMs with larger size could load more cells, which is possibly because it is easier for the cells to invade and attach on the inner surface of microcarriers with larger size. The cell behavior might be influenced by the curvature, surface roughness and microstructure cell of microcarriers, and the cell gene expressions on the two kinds of SSCMs were different in most of the cases. In view of the present and initial data, the SSCMs (180~280 μm) were found to be better for hFOB osteogenesis.

In summary, a novel cell microcarrier with open, hollow and shell-like structure was fabricated by a special surface crosslinking technique and subsequent dissolution of uncrosslinked material. The SSCMs show high cell loading efficiency and good biocompatibility, which can support favorable cell adhesion, rapid proliferation and controllable differentiation. The micro-structure, cytocompatibility, and cell affinity of SSCMs are specially developed for injectable perspective and evaluated with cell-loading tests. This suggests that SSCMs are competent for loading, expansion and delivery of therapeutic ADCs, especially for tissue regeneration purpose.

ACKNOWLEDGMENTS

This research was financially supported by grant AcRF Tier 1 RG 64/08, Ministry of Education, Singapore and NMRC/EDG/1001/2010, National Medical Research Council, Singapore.

REFERENCES

1. Wang C, Gong Y, Zhong Y, Yao Y, Su K, Wang DA. The control of anchorage-dependent cell behavior within a hydrogel/microcarrier system in an osteogenic model. Biomaterials. 2009;30:2259–69.
2. Wang C, Adrianus GN, Sheng N, Toh S, Gong Y, Wang DA. *In vitro* performance of an injectable hydrogel/microsphere based immunocyte delivery system for localised anti-tumour activity. Biomaterials. 2009;30:6986–95.
3. Hong Y, Gong Y, Gao C, Shen J. Collagen-coated polylactide microcarriers/chitosan hydrogel composite: Injectable scaffold for cartilage regeneration. J Biomed Mater Res A. 2008;85:628–37.
4. Häuselmann HJ, Masuda K, Hunziker EB, Neidhart M, Mok SS, Michel BA, *et al.* Adult human chondrocytes cultured in alginate form a matrix similar to native human articular cartilage. Am J Physiol Cell Physiol. 1996;271.
5. Drury JL, Mooney DJ. Hydrogels for tissue engineering: Scaffold design variables and applications. Biomaterials. 2003;24:4337–51.
6. Green DW, Leveque I, Walsh D, Howard D, Yang X, Partridge K, *et al.* Biomineralized polysaccharide capsules for encapsulation, organization, and delivery of human cell types and growth factors. Adv Funct Mater. 2005;15:917–23.
7. Tan J, Gemeinhart RA, Ma M, Mark Saltzman W. Improved cell adhesion and proliferation on synthetic phosphonic acid-containing hydrogels. Biomaterials. 2005;26:3663–71.
8. Malda J, Frondoza CG. Microcarriers in the engineering of cartilage and bone. Trends Biotechnol. 2006;24:299–304.
9. Frondoza C, Sohrabi A, Hungerford D. Human chondrocytes proliferate and produce matrix components in microcarrier suspension culture. Biomaterials. 1996;17:879–88.
10. Malda J, Van Blitterswijk CA, Grojec M, Martens DE, Tramper J, Riesle J. Expansion of bovine chondrocytes on microcarriers enhances redifferentiation. Tissue Eng. 2003;9:939–48.
11. Declercq HA, Gorski TL, Tielens SP, Schacht EH, Cornelissen MJ. Encapsulation of osteoblast seeded microcarriers into injectable, photopolymerizable three-dimensional scaffolds based on D, L-lactide and ε-caprolactone. Biomacromolecules. 2005;6:1608–14.
12. Wang C, Gong Y, Lin Y, Shen J, Wang DA. A novel gellan gel-based microcarrier for anchorage-dependent cell delivery. Acta Biomater. 2008;4:1226–34.
13. Gong Y, Wang C, Lai RC, Su K, Zhang F, Wang DA. An improved injectable polysaccharide hydrogel: modified gellan gum for long-term cartilage regeneration *in vitro*. J Mater Chem. 2009;19:1968–77.
14. Van Wezel AL. Growth of cell-strains and primary cells on microcarriers in homogeneous culture [17]. Nature. 1967;216:64–5.
15. Berry JM, Barnabé N, Coombs KM, Butler M. Production of reovirus type-1 and type-3 from vero cells grown on solid and macroporous microcarriers. Biotechnol Bioeng. 1999;62:12–9.

16. Bücheler M, Wirz C, Schütz A, Bootz F. Tissue engineering of human salivary gland organoids. Acta Oto Laryngol. 2002;122:541–5.
17. Harris SA, Enger RJ, Riggs BL, Spelsberg TC. Development and characterization of a conditionally immortalized human fetal osteoblastic cell line. J Bone Miner Res. 1995;10:178–86.
18. Wang DA, Williams CG, Yang F, Cher N, Lee H, Elisseeff JH. Bioresponsive phosphoester hydrogels for bone tissue engineering. Tissue Eng. 2005;11:201–13.
19. Chomczynski P, Sacchi N. The single-step method of RNA isolation by acid guanidinium thiocyanate-phenol-chloroform extraction: twenty-something years on. Nat Protoc. 2006;1:581–5.
20. Shi X, Wang Y, Ren L, Gong Y, Wang DA. Enhancing alendronate release from a novel PLGA/hydroxyapatite microspheric system for bone repairing applications. Pharm Res. 2009;26:422–30.
21. Mason PW, Lu ML, Jacobson BS. Cell substrate adhesion-induced redistribution of proteins among the apical, basal, and internal domains of the plasma membrane of HeLa cells spreading on gelatin. J Biol Chem. 1987;262:3746–53.
22. Wang C, Wang DA. An injectable, nanoaggregate-based system for mesenchymal stem cell (MSC) delivery: enhancement of cell adhesion and prevention of cytotoxicity. J Mater Chem. 2010;20:3166–70.
23. Wang C, Bai J, Gong Y, Zhang F, Shen J, Wang DA. Enhancing cell affinity of nonadhesive hydrogel substrate: the role of silica hybridization. Biotechnol Prog. 2008;24:1142–6.
24. Choi ST, Kim JH, Kang EJ, Lee SW, Park MC, Park YB, *et al.* Osteopontin might be involved in bone remodelling rather than in inflammation in ankylosing spondylitis. Rheumatology. 2008;47:1775–9.
25. Xue W, Krishna BV, Bandyopadhyay A, Bose S. Processing and biocompatibility evaluation of laser processed porous titanium. Acta Biomater. 2007;3:1007–18.
26. Rouahi M, Champion E, Hardouin P, Anselme K. Quantitative kinetic analysis of gene expression during human osteoblastic adhesion on orthopaedic materials. Biomaterials. 2006;27:2829–44.
27. Cer E, Gürpinar ÖA, Onur MA, Tuncel A. Polyethylene glycol-based cationically charged hydrogel beads as a new microcarrier for cell culture. J Biomed Mater Res B Appl Biomater. 2007;80:406–14.